Electronic Supplementary Material (ESI) for Journal of Materials Chemistry C.

SUPPORTING INFORMATION

Electron Injection and Scaffold Effect in Perovskite Solar Cells

Miguel Anaya,[1] Wei Zhang,[2,3] Bruno Clasen Hames,[4] Yuelong Li,[1] Francisco Fabregat-Santiago,[4] Mauricio E. Calvo,[1] Henry J. Snaith,[2,*] Hernán Míguez[1,*] and Iván Mora-Seró[4,*]

[1] Instituto de Ciencia de Materiales de Sevilla, CSIC, Avenida Américo Vespucio s/n, Isla de La Cartuja, 41092 Sevilla, Spain
[2] Department of Physics, University of Oxford, Clarendon Laboratory, Parks Road, Oxford, X1 3PU, United Kingdom.
[3] School of Chemistry, University of Lincoln, Beevor Street, Lincoln LN6 7DL, UK
[4] Institute of Advanced Materials (INAM), Universitat Jaume I, 12006 Castelló, Spain.

*Corresponding Authors: henry.snaith@physics.ox.ac.uk, h.miguez@csic.es, sero@fca.uji.es

	P	S	PMS1	PMS2	PMS3c	PMS3b	PMS3a
FTO (nm)	600±60	600±60	600±60	600±60	600±60	600±60	600±60
Nº TiO_2 layer	1	1	2	3	4	4	4
Total TiO_2 Thickness (nm)	35±3	35±3	70±6	105±9	140±12	140±12	140±12
Nº SiO_2 layer	0	1	1	2	3	3	3
Total SiO_2 Thickness (nm)	0	275±35	80±5	160±10	240±15	210±15	180±15
Perovskite capping (nm)	245±50	245±50	245±50	245±50	245±50	245±50	245±50
Spiro-OMeTAD (nm)	485±35	485±35	485±35	485±35	485±35	485±35	485±35
Au (nm)	50	50	50	50	50	50	50
Normalized Absorptance	1	0.77	0.95	0.92	0.91	0.91	0.92

Table S1: Number of the different layers and their thicknesses employed to fabricate the designed devices represented in the Fig. 1a. These data summarize a second set of samples (different for from the presented in the main text). We also include the normalized integrated absorptance, i. e. absorptance from 400 nm to 780 nm, of the different cells under investigation. Absorptances are normalized to reference devices P.

S1. Optical Characterization.

We have performed an extensive optical characterization using an integrating sphere. The spot size of the light beam is small enough to allow measurements in areas in which the gold layer is or is not present in the device.

Fig. S1a plots the absorptance of a reference P perovskite solar cell in which the light beam shines or not in the gold area.

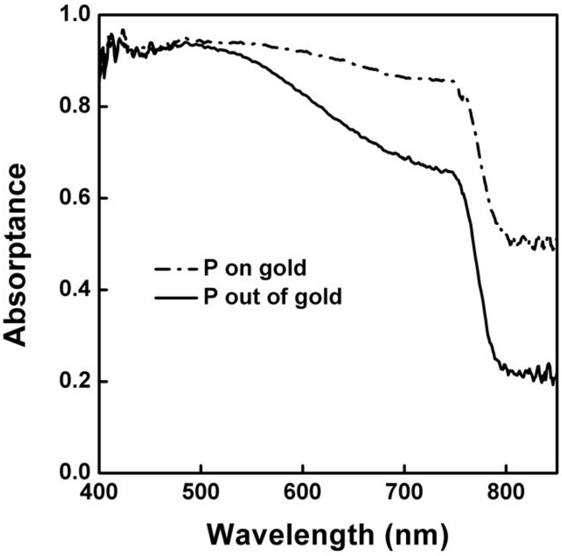

Fig. S1a: Absorptance of P reference cell in which light beam impinges (dashed-dot line) or not (solid line) in the gold contact.

It can be noticed that the absorptance spectrum corresponding to the measurement performed taking into account the Au film is clearly higher to that in which the effect of gold layer is not considered. This fact is caused by two phenomena: i) light parasitic absorption given in the gold layer, and ii) light absorbed by perovskite after being reflected by the gold layer. Therefore, from now on, we will present the absorption spectra obtained out of the area in which gold is deposited. It gives a better estimation of the total amount of perovskite deposited on each device (assuming that the absorption, i. e. thickness, of Spiro-OMeTAD and FTO remains constant between diverse samples). Fig. S1b shows a comparison between the absorptance spectra of the P samples from two different set of samples. These samples do not present any scaffold, being perovskite directly deposited on top of the TiO_2 blocking layer whose thickness is

27 nm and 35 nm, respectively, see Table 1 and Table S1. As expected, the amount of deposited perovskite does not depend on the TiO_2 blocking layer thickness.

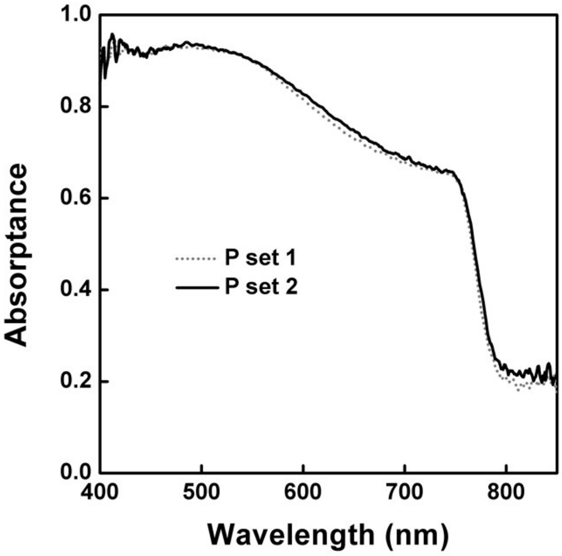

Fig. S1b: Absorptance of P reference samples.

Since the analysis can be extended to both conditions, we will focus the discussion on the set 2 of samples summarized in Table S1. Fig. S1c shows the absorptance and reflectance spectra for this set of samples. For samples with four TiO_2 layers with different total thickness of SiO_2 scaffold, the absorptance spectra (Fig. S1c left) are similar, but the reflectance peak redshifts (Fig. S1c right) when the thickness increases caused by the reflection of light due to the photonic effects provided by the multilayered scaffold.

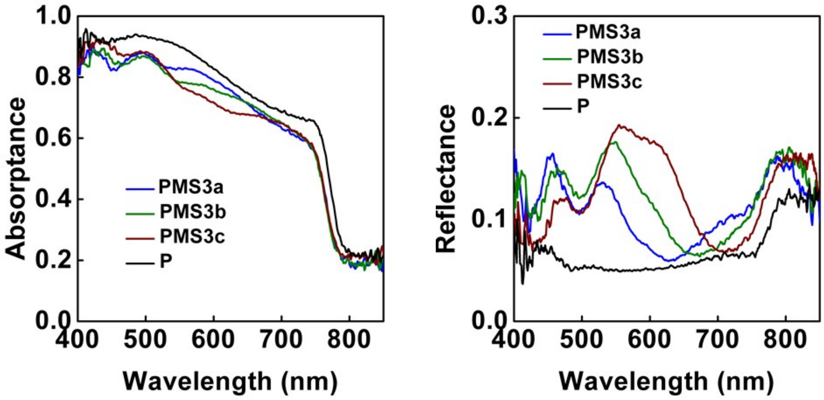

Fig. S1c: Absorptance of set 2 of samples. Samples with four TiO_2 layers but different total thickness of SiO_2 scaffold. **(left)** Absorptance; **(right)** Reflectance.

A comparable behavior is given when the number of layers in the scaffold is increased while preserving their individual thicknesses. Fig. S1d displays the absorptance and reflectance spectra for the devices whose scaffolds are constructed stacking 1, 2 and 3 successive SiO_2/TiO_2 bilayers on top of the of TiO_2 layer, keeping SiO_2 layers sandwiched by each two TiO_2 layers with the same thicknesses. Light absorption is reduced in the 400-to-600 nm range as the number of layers increases. It is a consequence of the stronger photonic effect giving rise a higher reflectance as the devices are fabricated with more layers. The amount of perovskite in these devices can be considered similar since the absorptance at 700 nm, where no photonic effects are foreseen, is almost the same.

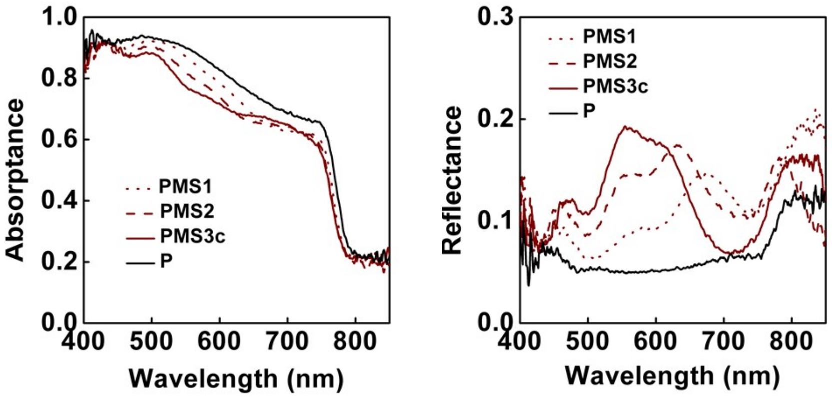

Fig. S1d: Absorptance of set 2 of samples. Samples with samples with different number of TiO_2 and SiO_2 layers. **(left)** Absortance; **(right)** Reflectance.

Finally, we show the transmittance spectra for the whole set 2 of samples, see Fig. S1e. These curves confirm all the discussion: light absorption within the different devices is very similar, and the small differences are explained by light reflection. This fact suggests that the amount of perovskite material present in the solar cells is comparable. Notice that S reference sample show a different behavior. In this case a thick mesoporous scaffold with no PMS is used to fabricate the device and the perovskite capping layer may be thinner. This effect can be debt to the porous nature of the underlying layer (a highly porous SiO_2 scaffold).

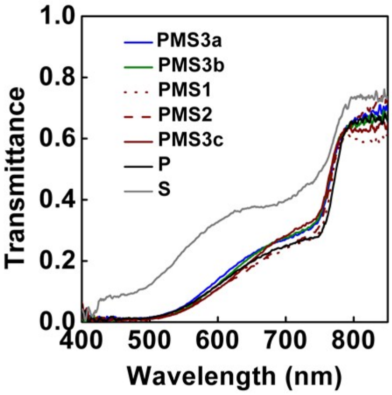

Fig. S1e: Transmitance of set of samples summarized in Table S1.

As it was pointed out above, the discussion can be extended to the set of samples summarized in Table 1. In order to draw a conclusion, we integrate the absorptance spectra for all the samples (from 400 nm to 780 nm) and we normalize them to the light absorption given in the reference cell P, depending on the set. The normalized absorptance calculated in this way is depicted in Table S2.

Set 1	**Sample**	**Integrated absorptance**	**Absorptance normalized to P**
	P	0.7972	1
	S	0.6653	0.835
	PMS3a	0.7608	0.954
	PMS3b	0.7478	0.938
	PMS3c	0.7873	0.988
	PMS2	0.7525	0.956
	PMS1	0.7572	0.950

Set 2	**Sample**	**Integrated absorptance**	**Absorptance normalized to P**
	P	0.8053	1
	S	0.6267	0.778
	PMS3a	0.7424	0.922
	PMS3b	0.7345	0.912
	PMS3c	0.7325	0.910
	PMS2	0.7413	0.921
	PMS1	0.7632	0.948

Table S2: Absorptance and normalized absorptance of the different devices in the 400-to780 nm spectral region. Normalization has been done with respect to P sample, depending on the set of solar cells.

S2. Transmission Electron Microscopy.

Fig. S2 displays a transmission electron microscopy image of the cross section of the PMS3c multilayer structure based perovskite solar cell. In Fig. S2 left, the different layers composing the device can be distinguished (from bottom to top): glass, FTO, perovskite infiltrated multilayer, perovskite capping layer, spiro-OMeTAD, and gold. On top of the cell it was deposited a platinum layer in order to avoid the degradation of the sample during FIB cutting. A detail of the SiO_2-TiO_2-SiO_2 interfaces is shown in Fig. S2 right. Characteristic perovskite crystal planes within the porous and amorphous SiO_2 nanoparticle layers can be observed. This fact confirms the good perovskite infiltration in the voids of SiO_2. On the other hand, no perovskite crystals seem to be present through the TiO_2 film.

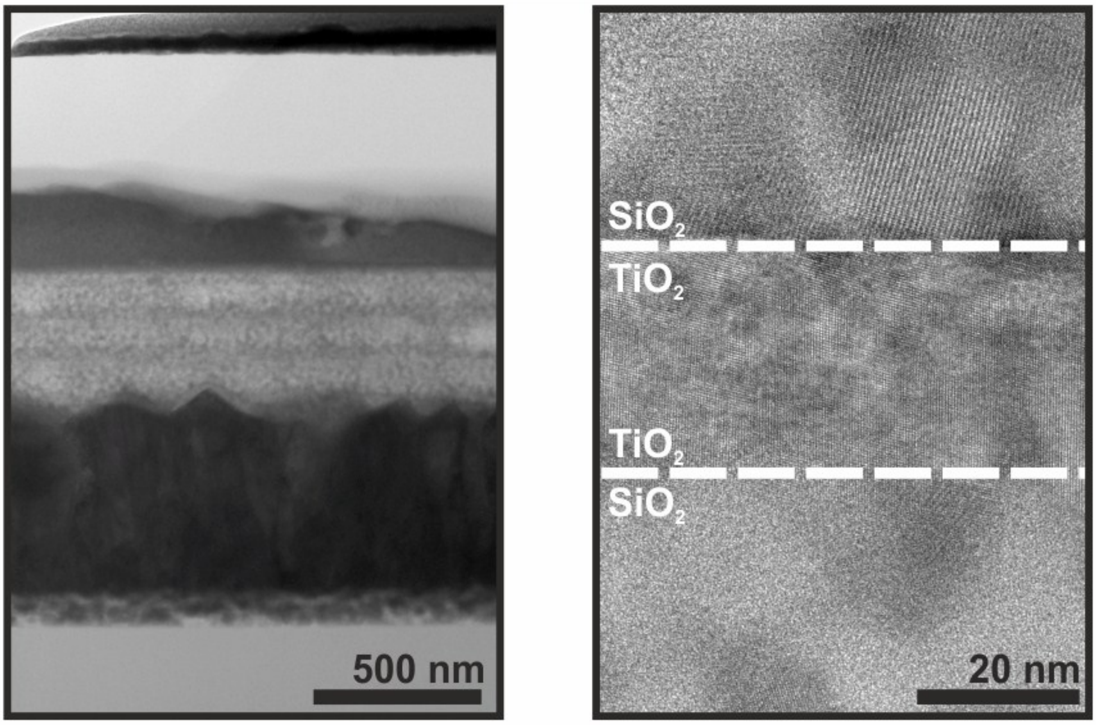

Fig. S2: TEM pictures of PMS3c sample. **(left)** complete cross section. **(right)** zoom of a TiO_2 layer sanwiched between two SiO_2 scaffold layers.

S3. J-V Curves.

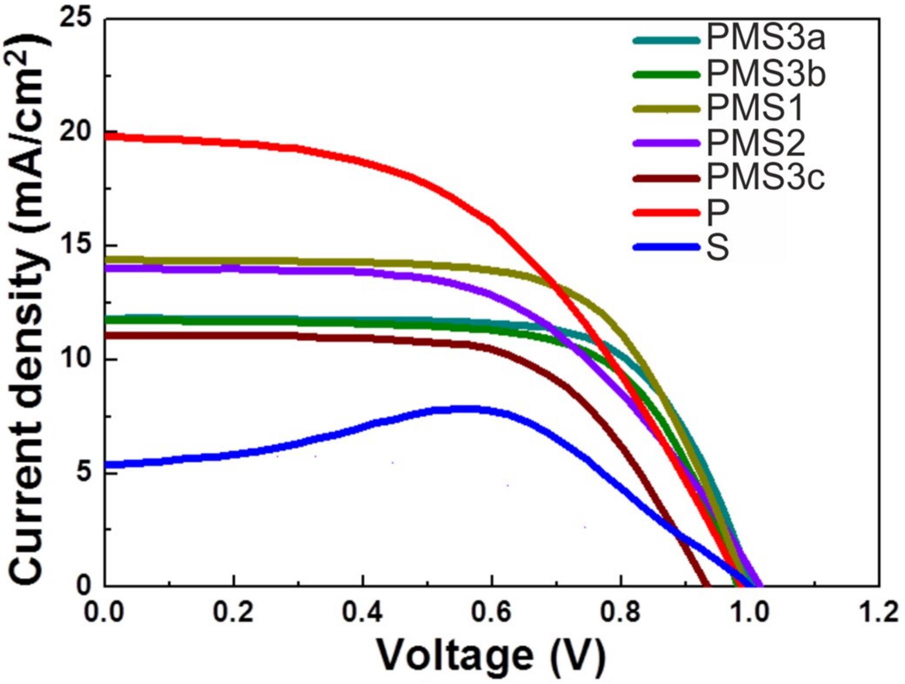

Fig. S3a: J-V curves under 1 sun illumination obtained for the set 2 of samples.

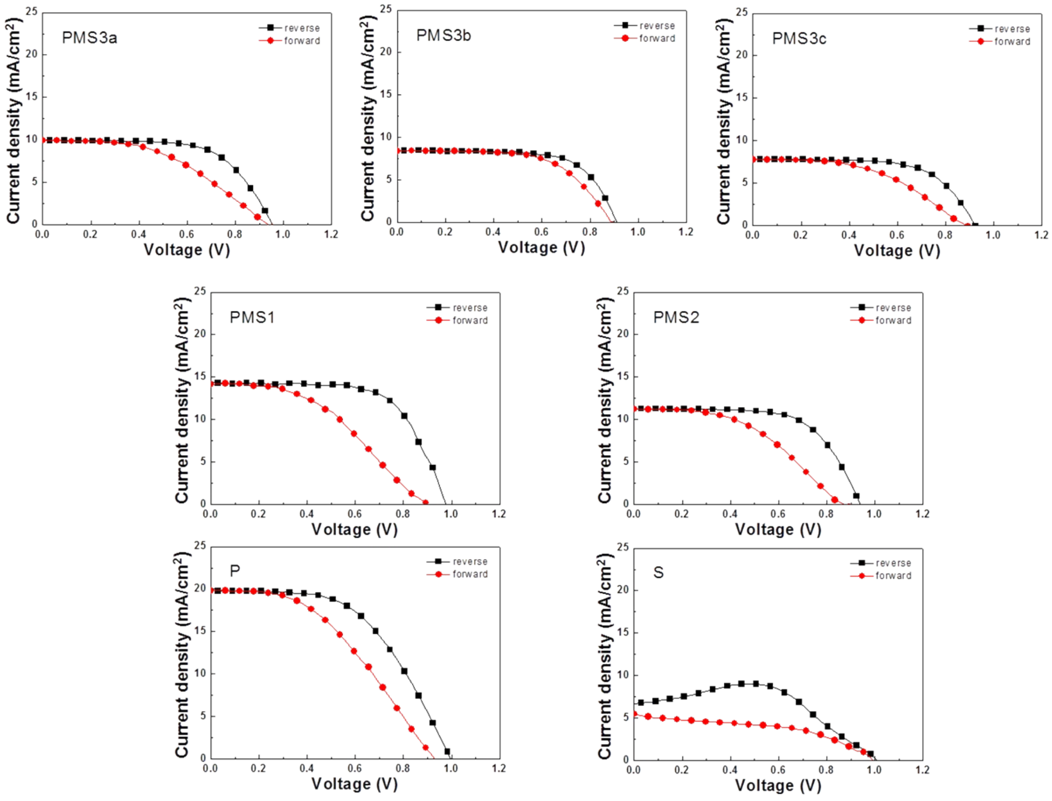

Fig. S3b: J-V curves under 1 sun illumination obtained for forward (from 0 V to V_{oc}) and reverse scans (from V_{oc} to 0 V) of the different devices from the set samples summarized in Table 1.

		Jsc (mA/cm^2)	Voc (V)	FF	Eff. (%)
PMS3a	reverse	9.91	0.953	0.640	6.09
	forward	9.93	0.923	0.462	4.27
PMS3b	reverse	8.40	0.923	0.665	5.19
	forward	8.39	0.894	0.601	4.54
PMS1	reverse	14.34	0.983	0.650	9.22
	forward	14.13	0.894	0.434	5.52
PMS2	reverse	11.28	0.923	0.650	6.82
	forward	11.23	0.864	0.458	4.48
PMS3c	reverse	7.80	0.923	0.640	4.64
	forward	7.75	0.894	0.472	3.29
P	reverse	19.84	0.983	0.539	10.56
	forward	19.82	0.923	0.428	7.89
S	reverse	6.67	1.013	0.741	5.04
	forward	5.45	0.983	0.464	2.50

Table S3: Performance parameters of the devices obtained from set samples summarized in Table 1 scanned under forward (from 0 V to V_{oc}) and reverse scans (from V_{oc} to 0 V) .

S4. Open Circuit Voltage Decay (OCVD) curves.

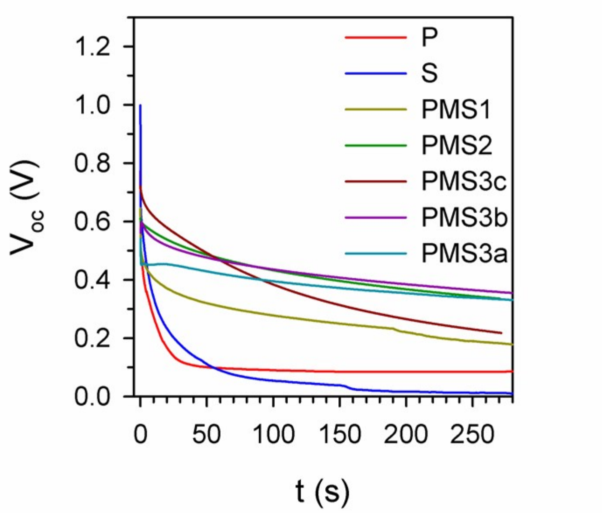

Fig. S4: OCVD curves under 1 sun illumination obtained by recording the V_{oc} after switch off the illumination. instantaneous relaxation time, τ_{ir}, plotted in Fig. 4 are obtained from this data using the relation: τ_{ir}= -V_{oc} dt/dV_{oc}.[1]

S5. Impedance Spectra Under Illumination at Short Circuit.

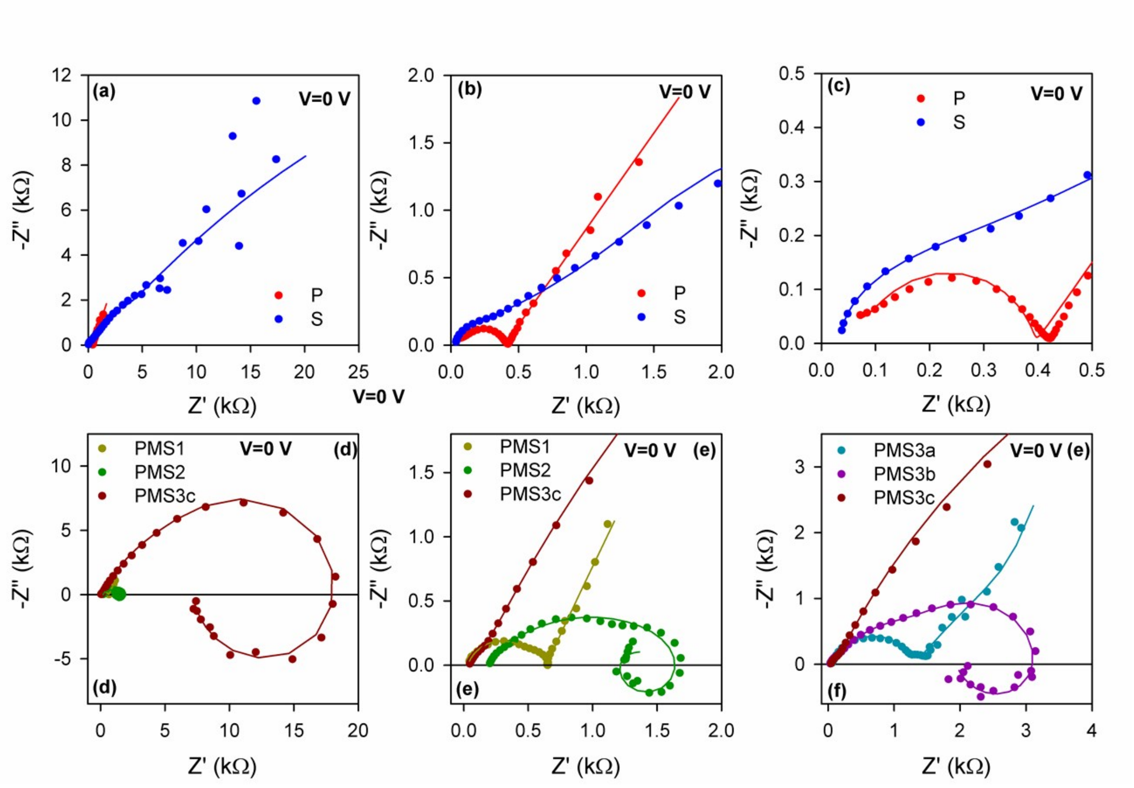

Fig. S5: Nyquist plot of impedance spectra obtained under illumination and with an applied bias of 0 V. (a) Reference samples P and S. (b) & (c) Zoom of (a). (d) Samples with different number of layer PMS1, PMS2 and PMS3c. (e) zoom of (d). (f) Samples with the same number of layers, PMS3a, PMS3b and PMS3c, but different thickness of the SiO_2 layers. Circle simbols in (a)-(e) represent the experimental point while solid lines are the fitting curves using equivalent circuits in Fig 5j and 5k, but with non-ideal elements, see Supporting Information S5.

Note that the effect herein reported is basically different to the negative capacitance observed at low frequency for $CH_3NH_3PbI_3$ top-contacted with interdigitated contacts separated 50µm, which has been associated to a solid state electrochemical reaction. In our case, a complete loop is observed and not just a negative capacitance. In addition, the effect remains at intermediate frequencies.

S6. Ideal vs. Non-Ideal Elements in Equivalent Circuits.

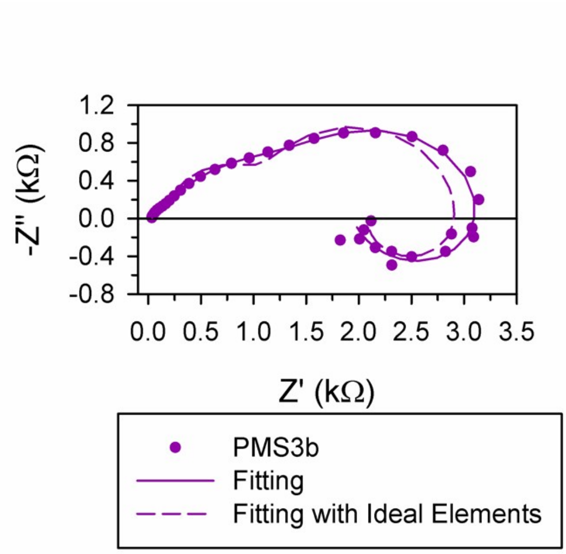

Fig. S6: Nyquist plot of impedance spectra of sample PMS3b under illumination and with an applied bias of 0.7 eV. Circles represent the experimental points, dashed line the fitting using equivalent circuit from Fig. 5k and solid line fitting using equivalent circuit from Fig. 5k but using constant phase elements instead of ideal capacitors and inductance.

S7. Comparison of the Inductive Value Between Samples Corresponding to Different Sets.

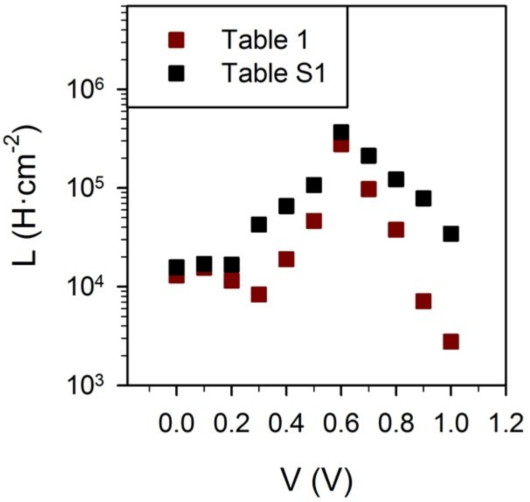

Fig. S7: Inductance obtained for the fit of impedance spectra under illumination obtained for sample PMS3c of the two different set of samples, the one summarized in Table 1 and the summarized in Table S1. The value has been obtained using the equivalent circuit plotted in Fig. 5k.

S8. Resistance Values Obtained from the Fitting of the Impedance Spectra for Set of Samples Summarized in Table S1.

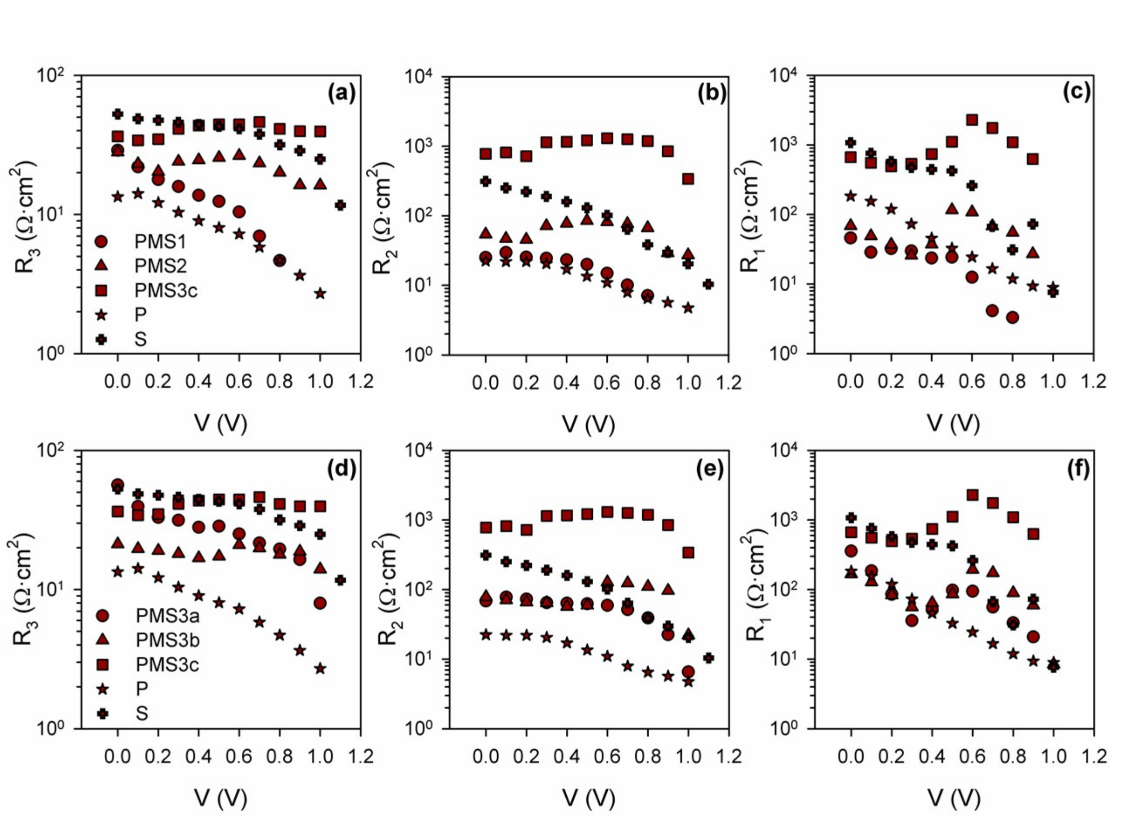

Fig. S8: Resistance values obtained from the fitting of impedance spectra from sample set 2 using equivalent circuit plotted in Fig. 5j and 5k. (a) R_3; (b) R_2 and (c) R_1 for reference samples and PMS samples with different number of TiO_2 layers. (d) R_3; (e) R_2 and (f) R_1 for reference samples and PMS samples with the same number of TiO_2 layer, but different thickness of the SiO_2 layers.

S9. C_{bulk} and C_2 Values Obtained from the Fitting of the Impedance Spectra for the Set of Samples Summarized in Table 1.

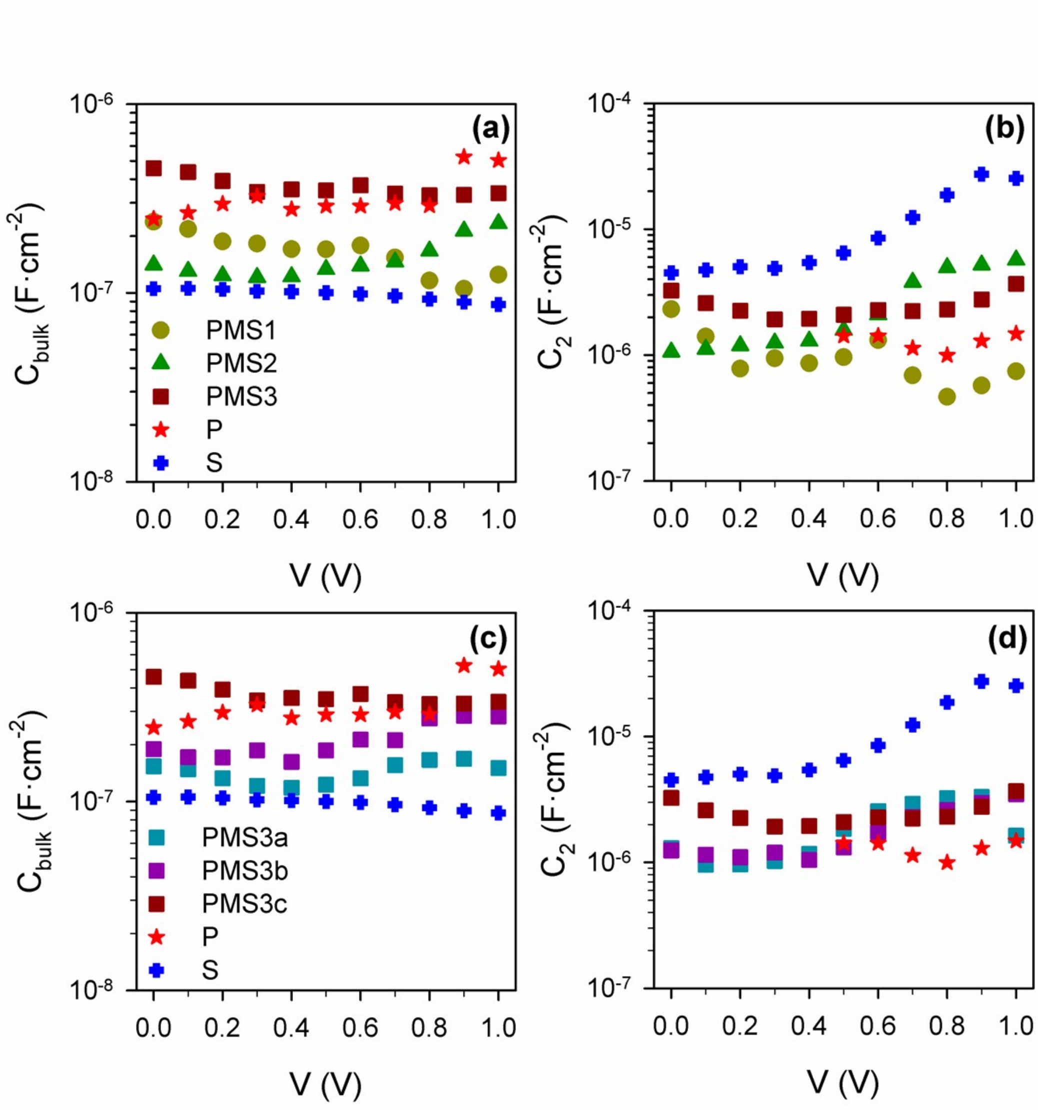

Fig. S9: Capacitance values obtained from the fitting of impedance spectra using equivalent circuit plotted in Fig. 5j and 5k. **(a)** C_{bulk} and **(b)** C_2 for reference samples and PMS samples with different number of TiO_2 layers. **(d)** C_{bulk} and **(e)** C_2 for reference samples and PMS samples with the same number of TiO_2 layer, but different thickness of the SiO_2 layers..

S10. Capacitance Values obtained from the Fitting of the Impedance Spectra for the set of Samples Summarized in Table S1.

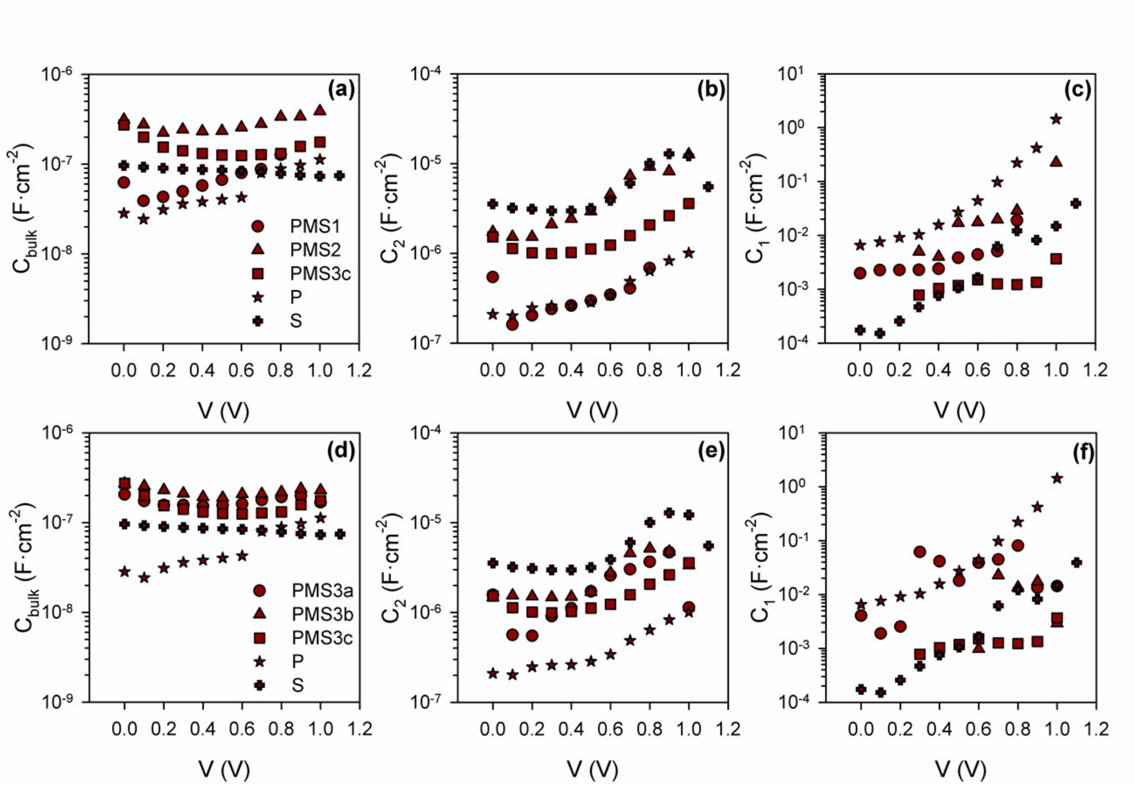

Fig. S10: Capacitance values obtained from the fitting of impedance spectra from sample set 2 using equivalent circuit plotted in Fig. 5j and 5k. (a) C_{bulk}; (b) C_1 and (c) C_2 for reference samples and MS samples with different number of TiO_2 layers. (d) C_{bulk}; (e) C_1 and (f) C_2 for reference samples and MS samples with the same number of TiO_2 layer, but different thickness of the SiO_2 layers..

References

1. L. Bertoluzzi, R. S. Sanchez, L. Liu, J.-W. Lee, E. Mas-Marza, H. Han, N.-G. Park, I. Mora-Sero and J. Bisquert, *Energy & Environmental Science*, 2015, 8, 910-915.